Published online 31 May 2014 *Nucleic Acids Research, 2014, Vol. 42, No. 12* ***7935–7946***
doi: 10.1093/nar/gku494

A highly processive topoisomerase I: studies at the single-molecule level

Marcin Jan Szafran[1,*], Terence Strick[2,*], Agnieszka Strzałka[1], Jolanta Zakrzewska-Czerwińska[1,3] and Dagmara Jakimowicz[1,3]

[1]Faculty of Biotechnology, University of Wrocław, Joliot-Curie 14A, 50-383 Wrocław, Poland, [2]Institut Jacques Monod, CNRS UMR 7592, University Paris Diderot, Sorbonne Paris Cité, F-75205 Paris, France and [3]Ludwik Hirszfeld Institute of Immunology and Experimental Therapy, Polish Academy of Sciences, Weigla 12, Wrocław, 53-114, Poland

Received February 14, 2014; Revised May 16, 2014; Accepted May 16, 2014

ABSTRACT

Amongst enzymes which relieve torsional strain and maintain chromosome supercoiling, type IA topoisomerases share a strand-passage mechanism that involves transient nicking and re-joining of a single deoxyribonucleic acid (DNA) strand. In contrast to many bacterial species that possess two type IA topoisomerases (TopA and TopB), *Actinobacteria* possess only TopA, and unlike its homologues this topoisomerase has a unique C-terminal domain that lacks the Zn-finger motifs characteristic of type IA enzymes. To better understand how this unique C-terminal domain affects the enzyme's activity, we have examined DNA relaxation by actinobacterial TopA from *Streptomyces coelicolor* (*Sc*TopA) using real-time single-molecule experiments. These studies reveal extremely high processivity of *Sc*TopA not described previously for any other topoisomerase of type I. Moreover, we also demonstrate that enzyme processivity varies in a torque-dependent manner. Based on the analysis of the C-terminally truncated *Sc*TopA mutants, we propose that high processivity of the enzyme is associated with the presence of a stretch of positively charged amino acids in its C-terminal region.

INTRODUCTION

In prokaryotes, and similarly in eukaryotes, deoxyribonucleic acid (DNA) needs to be highly compacted to fit the space limited by the cell size (1–4). Although the chromosome is highly condensed within a cell, it also has to be accessible for dynamic processes such as replication, transcription, recombination and segregation, the proper execution of which is dependent on spatial DNA structure. Local chromosome organization is exerted by nucleoid-associated proteins and histones in prokaryotes and eukaryotes, respectively, whilst global compaction is induced by condensins (SMC) (5–7). However, in most cases negative supercoiling is the first step of DNA compaction which within the cell is maintained by enzymes called topoisomerases.

Topoisomerases act by removing or introducing supercoils into the DNA molecule. The two evolutionarily and functionally distinct types—type I and type II (8,9)—exhibit different reaction mechanisms. Whilst type II topoisomerases (e.g. gyrase) catalyze cleavage and religation of both DNA strands, type I topoisomerases cut a single strand. Formation of an intermediate covalently linked to DNA allows for topological manipulation of the DNA prior to religation. In the case of type I topoisomerases, transfer or rotation of the intact strand occurs due to topological tension, and so the relaxation they perform does not require adenosine triphosphate (bacterial reverse gyrase is a notable exception). Type I topoisomerases are further divided into subtypes IA, IB and IC, according to the origin, the differences in amino acid sequence and/or the relaxation mechanisms. Whilst topoisomerases of type IB are present in eukaryotes, poxviruses and a few bacteria species [their presence in bacteria may be the effect of horizontal gene transfer (10)], topoisomerases of type IA and IC are characteristic of prokaryotes and archaea. Topoisomerases IB and IC form linkage with the 3′-end of DNA and remove several positive or negative supercoils (L_k, linking number; the number by which one DNA helix contacts with the second one and which cannot be altered without strand breakage) per cleavage/religation cycle using a constrained swiveling mechanism, whilst topoisomerases IA (TopA and TopB) form a 5′-phosphotyrosine intermediate and can relax only one negative supercoil per cleavage/religation event using an enzyme-bridged strand passage mechanism (11–13).

The similarity between TopA and TopB proteins manifests itself mostly in the conserved N-terminal region, containing a TOPRIM (*top*oisomerase-*prim*ase) domain

*To whom correspondence should be addressed. Tel: +48 71 375 2926; Fax: +48 71 375 2608; Email: marcin.szafran@uni.wroc.pl
Correspondence may also be addressed to Terence Strick. Tel: +33 1 57 27 80 20; Fax: +33 1 57 27 81 01; Email: strick.terence@ijm.univ-paris-diderot.fr

and the catalytic tyrosine residue required for the *trans*-esterification reaction (14,15). Although TopA and TopB share the same overall mechanism of supercoil removal, they differ in details at both the structural and mechanistic levels. TopA homologues contain a long C-terminal domain with zinc-finger motifs that are absolutely required for DNA binding and relaxation, whilst TopB homologues possess a short C-terminal domain lacking those structures. The difference in the structure of TopA and TopB reflects their cellular function and the mechanism by which they relax supercoiled DNA. Whilst *Escherichia coli* TopA removes negative supercoils efficiently and plays a major role in maintaining the appropriate superhelical density of the chromosome, TopB relaxes negatively supercoiled DNA more slowly and pauses between each relaxation burst (16). However, TopB is more efficient in decatenating single-stranded DNA rings due to the presence of a structural motif named the decatenation loop (17,18). Thus, *in vivo* TopB may be involved in several types of DNA transactions, but its cellular role remains still unclear.

Although many bacterial species, in particular rapidly growing ones, possess genes encoding both type IA topoisomerases, the linear chromosome of mycelial, multigenomic and sporulating bacteria, *Streptomyces coelicolor* contains only one gene encoding topoisomerase of type I (*Sc*TopA) (19) that is essential for cell viability (20,21). In contrast to other TopA homologues, the enzyme identified in *S. coelicolor* (20), as in other *Actinobacteria* [(22,23) and Supplementary Figure S1], contains a very long C-terminal domain lacking zinc fingers but encompassing the stretch of positively charged amino acids. Thus, it exhibits poor homology to either TopA or TopB families and seemingly belongs to an evolutionarily distinct branch of enzymes (Supplementary Figure S1). The earlier studies (22,24) on topoisomerase I from *Mycobacterium smegmatis* (*Ms*TopA) suggested its specificity towards recognized sequences and high processivity of DNA relaxation. The unusual features of the actinobacterial TopA proteins sequence prompted us to analyse characteristics of *Sc*TopA-dependent relaxation using single-molecule magnetic tweezer and classical agarose gels. Both strategies gave us direct access to important biological parameters of the enzyme such as velocity and processivity, allowing us to describe in detail the relaxation process. In particular, we show that *Sc*TopA is characterized by an extremely high processivity not reported earlier for any known topoisomerase of type I which is correlated with the presence of a stretch of positively charged amino acids in C-terminus.

MATERIALS AND METHODS

In silico analysis

All similarity analyses were performed using Basic Local Alignment Search Tool. Amino acid sequences of bacterial topoisomerases type IA were retrieved from UniProtKB Protein Knowledgebase (www.uniprot.org). Phylogenetic analysis of bacterial topoisomerases was prepared using MEGA5.1 software and MUSCLE algorithm for multiple sequence alignment. The guide tree was calculated using the neighbour-joining Method. Secondary structures of *Sc*TopA and *Ec*TopA, respectively, were predicted using GOR, HNN and SOPMA algorithms (www.expasy.org/tools).

Protein overexpression and purification

Topoisomerase I (*Sc*TopA) was overproduced using the construct pET*topA* and purified as described earlier (21). To overproduce the truncated versions of *Sc*TopA protein, the construct pET*topA* was modified by λRed-mediated recombination with the use of the apramycin resistant cassette amplified using oligonucleotides topA_delC_FW and topA_delC_RV (for *Sc*TopAΔC carrying 343-aa C-terminal deletion) and topA881_FW and topA_delC_RV (for *Sc*TopA881 carrying 71-aa C-terminal deletion) yielding pET*topA*ΔC and pET*topA*881, respectively. Both *Sc*TopA-truncated versions were subsequently overexpressed in *E. coli* BL21 strain, purified and tested for nuclease contamination; 250 ng of the purified protein was incubated 24 h in 37°C with 200 ng of supercoiled pUC19 plasmid in 25-mM NaH_2PO_4 pH 8.1, 150-mM NaCl, 5% glycerol, 10-mM $MgCl_2$ and supplemented with 1-mg/ml bovine serum albumin (BSA). After this time DNA was extracted using phenol:chlorophorm:isoamyl alcohol (25:24:1). DNA was analysed by standard gel electrophoresis in 1% agarose in 1x Tris-borate-EDTA (TBE) buffer to confirm no nicking occurred.

Topoisomerase relaxation assay

A 20-μl mixture containing 200 ng of negatively supercoiled plasmid, 10-mM $MgSO_4$, 1-mg/ml BSA, 50-mM NaH_2PO_4 pH 8.1, 150-mM NaCl, 5% glycerol and increasing concentration of *Sc*TopA protein (0–500 nM) was incubated in 37°C for the time indicated. To compare the activity of *Sc*TopA and *Sc*TopA881 proteins, we incubated 200 ng of pUC19 plasmid in the presence of 100-nM enzyme for up to 60 min. The reaction was stopped by addition of 1.5 μl of 0.5-M ethylenediaminetetraacetic acid (EDTA). DNA was subsequently extracted by vortexing with 1 volume of phenol:chlorophorm:isoamyl alcohol (25:24:1). DNA was resolved in 1% agarose in Tris-acetate-EDTA (TAE) buffer for 14–16 h at low voltage (2 V/cm). Topoisomers distributions were visualized by staining in ethidium bromide/TAE solution at room temperature for 30 min. Band intensities and relaxation profiles were analysed on Typhoon 8600 Imager using software provided by the producer. To estimate the kinetic parameters (K_m and V_{max}), 10 ng of *Sc*TopA (5 nM) or 150 ng of *Sc*TopA881 mutant truncated in positively charged C-terminus (75 nM) was incubated with increasing amount of pUC19 plasmid (100–2500 ng) carrying in each DNA molecule 8–10 supercoils that are the substrate for *Sc*TopA. The V_{max} parameters were subsequently linearly extrapolated to the same enzyme concentration allowing their comparison. The reaction was stopped at different stages (30–120 s), plasmid was resolved and visualized as described above. To estimate the initial velocity (V_0), the intensity of the band corresponding to the supercoiled form was measured using ImageJ2x Software and compared with non-relaxed plasmid $-R$ value (after time 0 s) according to the protocol described by Xu and Leng (25). V_0 was

calculated from linear decrease of supercoiled form; $V_0 = [\text{scDNA}] \times (1 - R) \times 1/t$, where t is the reaction time. Obtained values were fitted to the Michaelis–Menten model using R Software and drc package.

Single-molecule experiments: sample preparation, magnetic trap calibration and data analysis

Topoisomerase I activity can be assayed in real time on mechanically supercoiled, extended DNA as an increase in DNA extension resulting from topological relaxation of plectonemic supercoils. Controlling the extending force on negatively supercoiled DNA makes it possible to alter the balance between plectonemic and denatured states, making the appearance of denatured states more frequent by increasing the force. The analysis of *Sc*TopA relaxation mechanism was performed for a broad range of DNA substrates (2–51 kb) in Hepes buffer (25-mM Hepes-KOH pH 8.0, 150-mM NaCl, 10-mM $MgSO_4$, 1-mg/ml BSA 0.1% Tween), in which the same activity of *Sc*TopA was observed as in bulk experiment. For single-molecule experiments, DNA fragments to be nanomanipulated were cut with XbaI and SacI, gel purified and subsequently ligated with purified 1-kb DNA labels XbaI-biotin and SacI-digoxigenin, respectively. One-kilobase DNA labels were prepared by polymerase chain reaction-based incorporation of either 2'-deoxyuridine-5'triphosphate-biotin (dUTP-biotin) or dUTP-digoxigenin into 1-kb fragments bearing an appropriate restriction site according to the protocol described previously by Revyakin *et al.* (26). The 11-kb DNA built in this manner is based on the Charomid 9–11-kb DNA; 2-kb DNA is a fragment of the *S. coelicolor* chromosome (*oriC* proximal region). The 17-kb DNA is pFX357 (a kind gift from Dr François-Xavier Barre), and 51-bp molecules are occasional trimers of pFX357 observed in the magnetic trap to be ∼16 μm in length. These longer molecules were prepared by ligating AatII/XhoI-digested pFX357 to 1-kb DNA fragments bearing an AatII or XhoI site and labelled with multiple biotin or digoxigenin groups, respectively, as above.

Subsequently, labelled DNA fragments were attached first to streptavidin-coated magnetic beads (Dynal MyOne, Life Technologies), then to an antidigoxigenin-coated glass flow cell and placed on a home-built magnetic trap running the PicoTwist software suite. Preparation of flow cells for all micromanipulation experiments and measurement of stretching force were performed according to the procedure described in (26). The flow cell was placed on a magnetic trap instrument based on an inverted microscope. Here the magnetic beads were acted upon by a magnetic field gradient generated by a pair of rare earth magnets located above the sample. The gradient generated a vertical stretching force on the bead. The stretching force could be increased by moving the magnets closer to the sample, and rotation of the magnets caused the bead to rotate in lock-step register (Figure 1A). The DNA extension was measured in real time (30 Hz) by analysing the position of the bead above the surface using nm-resolution particle tracking algorithms.

To make certain whether the bead was tethered to the surface via a single, intact DNA molecule, the DNA was extended at a low force ($F = 0.3$ pN) and subsequently supercoils were introduced by rotating the magnet on the tweezers. In these conditions, the extension of a single supercoiled DNA molecule should decrease with the number of magnet rotations at a rate of ∼50–55 nm/turn. Nicked molecules that did not show this characteristic correlation between DNA length and the number of rotations were omitted from subsequent analysis. Similarly, beads attached to more than one DNA molecule could also be omitted from subsequent analysis based on characteristically peaked extension versus supercoiling curves (27).

The analysis of the influence of supercoiling on a DNA molecule attached to a magnetic bead has shown that DNA can be extended by low forces and negatively supercoiled by several percent without provoking extensive DNA denaturation. At low stretching force ($F \sim 0.3$ pN in the salt conditions used here) negatively supercoiled DNA adopts a stable, plectonemic form. When such DNA is stretched with higher force ($F \sim 0.5$ –1 pN in the salt conditions used here), the equilibrium between plectonemic and denatured states is shifted towards denatured states and locally single-stranded regions appear (28). On the other hand, for equally positively supercoiled DNA and within the force range discussed here, plectonemic supercoiling dominates throughout and denatured states are repressed. Unless stated otherwise, experiments were carried out at $F = 0.3$ pN.

RESULTS

*Sc*TopA relaxes only negatively supercoiled DNA in a force- and torque-dependent manner

Comparison of *Sc*TopA with its homologues from other bacteria revealed the unusual presence of a long C-terminal domain lacking zinc fingers but terminated with a stretch of positively charged amino acids (Supplementary Figure S1A–C), thus suggesting possible differences in the DNA binding and relaxation activity of *Sc*TopA in comparison to, for instance, the enzyme from *E. coli* (*Ec*TopA). The sequence analysis and the bulk assays of *Sc*TopA activity, which suggested rapid supercoil removal [(21) and see also Figure 7A] prompted us to analyse the properties of *Sc*TopA in single-molecule experiments using magnetic tweezers. In these experiments, the DNA substrates are tethered between a glass surface and a 1-μm magnetic bead and manipulated as described in the Materials and Methods section (see Figure 1A and B).

We first analysed the relaxation of positively and negatively supercoiled 2-kb DNA in the presence of *Sc*TopA (5 nM) at two stretching forces (low force $F = 0.3$ pN, medium force $F = 0.5$ pN). When positive supercoils were introduced into the DNA molecule, no DNA relaxation by *Sc*TopA was observed either at low or at medium extending forces (Figure 1C and Supplementary Figure S2). On the other hand, when the DNA molecule was negatively supercoiled its relaxation in the presence of *Sc*TopA could be detected (Figure 1C).

Next, we analysed the kinetics of onset of supercoil relaxation using two related parameters: the initial time lag (ITL), defined as the time between mechanical introduction of supercoils into DNA and the first relaxation event caused by *Sc*TopA activity, and the number of molecules for which no relaxation has been observed after 800 s (the maximal

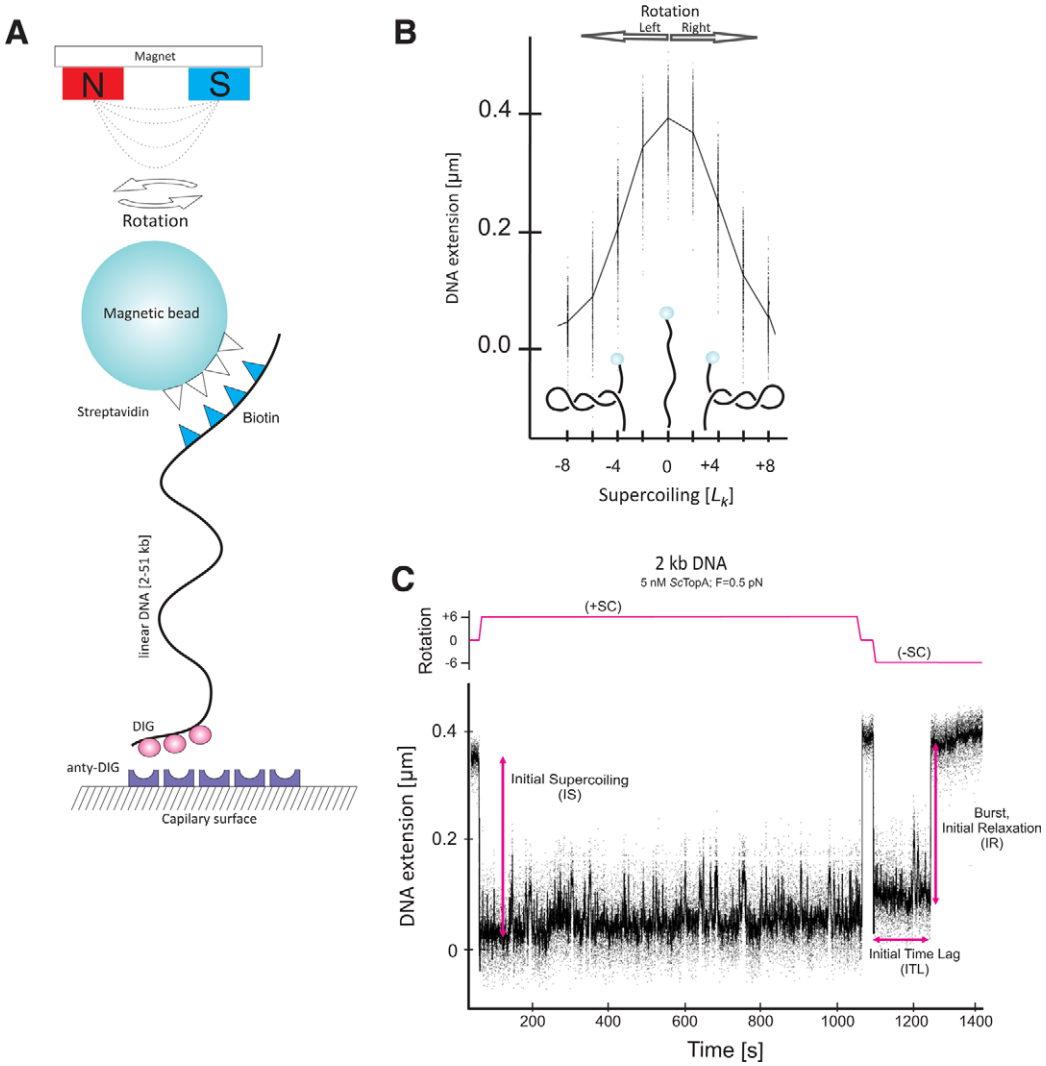

Figure 1. Single-molecule assay for analysis of *Sc*TopA relaxation activity. (**A**) The scheme of the experiment. (**B**) Extension versus supercoiling curve for 2-kb dsDNA extended by a force $F = 0.3$ pN. (**C**) Time-trace of *Sc*TopA activity acting on 2-kb dsDNA for positive (+SC) and negative (−SC) supercoiling.

recording time). Histograms of individual ITLs show that they are distributed according to single-exponential statistics (Figure 2A). At the medium force ($F = 0.5$ pN), the ITL was shorter than 100 s for 83% (Figure 2A) of molecules and less than 2% of molecules were not relaxed after 800 s (Figure 2A, grey bar). At the low stretching force ($F =$ 0.3 pN), the number of relaxed DNA molecules decreased dramatically: the ITL was shorter than 100 s for only 26% of observed beads (Figure 2, inset) and almost 50% of observed molecules were not relaxed after 800 s (Figure 2A, inset, grey bar). Thus, we observed that relaxation of negatively supercoiled molecules by *Sc*TopA occurred more frequently at a medium extending force ($F = 0.5$ pN) than at a low extending force ($F = 0.3$ pN). These experiments thus show that *Sc*TopA, in a manner similar to *Ec*TopA, exhibits the ability to relax supercoiled DNA in a force- and torque-dependent manner.

*Sc*TopA removes several supercoils independently of enzyme concentration

Although in experiments at the single-molecule level *Sc*TopA exhibited substrate preference characteristic of the TopA family, we also observed the atypical occurrence of full relaxation of DNA molecules in a single relaxation burst (i.e. the relaxation event consists in a continuous increase in DNA extension until nearly maximal extension). The relaxation of DNA molecules by removal of several supercoils in a rapid burst may result from the concurrent action of several enzyme molecules, although this is statistically unlikely given the long ITLs observed earlier. To further rule this possibility out, we analysed the relaxation of 2-kb DNA at different *Sc*TopA concentrations and plotted the correlation between initial supercoiling (IS, the length by which the molecule is shortened as a result of magnet rotation) and initial relaxation (IR, the length by which DNA extension increases as a result of *Sc*TopA activity during the first burst of relaxation). Similar values of IS and IR parameters (IS ∼ IR; Figure 3, marked with a dotted line)

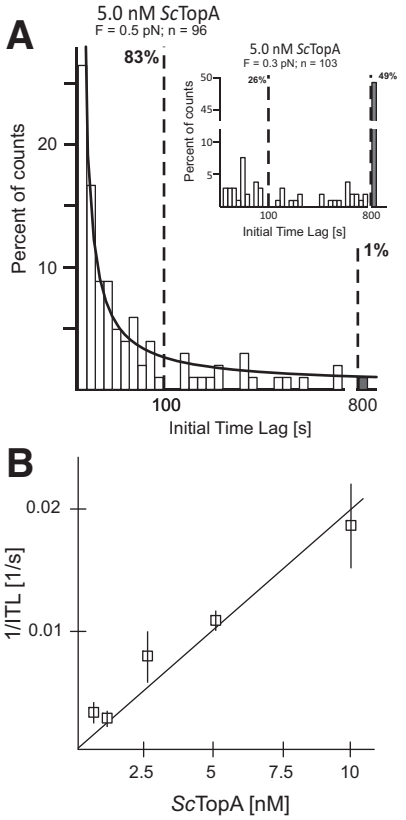

Figure 2. Force and concentration dependence of the rate at which *Sc*TopA initiates DNA relaxation. (**A**) The initial time lag (ITL) for *Sc*TopA activity displays a single-exponential distribution and decreases with increasing extending force. Histograms show the distribution of ITL values measured for 5-nM *Sc*TopA and DNA extended by a force $F = 0.5$ pN (main panel) compared to ITL values measured at low extending force (inset, $F = 0.3$ pN). The lower extending force resulted in a near abolition of DNA relaxation events and a dramatic elevation of the number of unrelaxed molecules (grey bars in both panels). The number of molecules analysed (n) is shown at the top of each panel. The line corresponds to a single-exponential fit to the data obtained at 5 nM and for which unrelaxed molecules are proportionally very infrequent, giving a mean ITL = 29 s. Dashed vertical bars indicate the fraction of molecules relaxed within 100 s and 800 s, respectively. (**B**) *Sc*TopA activity initiates more rapidly as concentration increases. The rate of initiation 1/ITL is obtained at each concentration by fitting a single-exponential decay to the cumulative probability distribution of individual ITLs. The cumulative probability distribution allows one to include in the analysis the unrelaxed DNA molecules (which become more frequent at lower concentrations), and by fitting at short timescales the characteristic decay time of the distribution is obtained. For 0.5 nM, $n = 43$ of which 15 are molecules unrelaxed after 800 s; for 1 nM, $n = 39$ of which 12 are unrelaxed molecules; for 1 nM, $n = 59$ of which four are unrelaxed molecules; statistics for 5 nM are given in (A); and for 10 nM, $n = 42$ of which one is an unrelaxed molecule. Error bars represent SEM obtained from the single-exponential fit.

mean nearly complete DNA relaxation in a single relaxation burst, whilst IR < IS and IR = 0 correspond to relaxation in more than one burst and no relaxation at all, respectively. We noticed that *Sc*TopA at a high concentration (2.5–5.0 nM) relaxed a large fraction of molecules in one burst (63.3% and 67.9%, respectively). Interestingly, decreasing the concentration of *Sc*TopA did not lead to an increase in the fraction of molecules in the IR<IS category, corresponding to relaxation of DNA supercoils in multiple bursts. Instead, using lower *Sc*TopA concentrations (0.5–1.0 nM) resulted in an increase of the fraction of molecules which remained supercoiled, although there was still a significant fraction of molecules that were relaxed in a single burst (41.2% and 44.1%, respectively). Thus, the removal of many supercoils in one relaxation event even at low enzyme concentration is most likely carried out by a single *Sc*TopA molecule or its active multimer, rather than several *Sc*TopA molecules/complexes acting independently.

We next estimated the rate of onset of supercoil relaxation by considering both the ITL and the number of molecules that have not been relaxed at the end of the experiment. We thus considered an initial population consisting of all of the initially supercoiled DNA molecules and calculated its decay over 800 s to a final state where only the unrelaxed molecules remain. We fit this decay to a single-exponential distribution and obtain the rate as the inverse of the decay time and plot the rate as a function of concentration (Figure 2B and Supplementary Figure S3). The rate of onset of supercoil relaxation increased linearly with topoisomerase I concentration, suggesting that diffusion is limiting in this concentration range and reinforcing the idea that these relaxation events result from the activity of a single topoisomerase I molecule/complex. From these measurements, we estimated an apparent first-order binding rate for the 2-kb DNA of about 2×10^6/M·s, consistent with diffusion-limited activity.

To summarize, the magnetic trap experiments indicate that DNA subjected to *Sc*TopA action remains supercoiled until the enzyme removes nearly all supercoils in a single burst of activity. This explains the apparent bimodal distribution of topoisomers observed in gel-based measurements of *Sc*TopA activity. Although increasing *Sc*TopA concentration shortened the initial time necessary for enzyme activity to be observed, it did not affect enzyme activity itself.

*Sc*TopA preferentially relaxes DNA in a single relaxation burst

Our observation that *Sc*TopA activity can remove nearly all DNA supercoils in a single burst of activity prompted us to check if this was still the case for longer DNA fragments that can accommodate more extensive supercoiling. Thus, we measured the number of relaxation bursts required to remove nearly all supercoils from the DNA substrates in the 2–51-kb range. For the 2-kb DNA substrate, the vast majority of molecules were relaxed in a single burst of *Sc*TopA activity (~63%). For the remaining third of DNA molecules relaxation occurred in multiple bursts separated by long pauses (Figure 4B, inset); 26% and 11% of all relaxation time-traces showed one and two pauses, respectively, corresponding to two or three relaxation bursts (Figure 4A). Interestingly, when we used longer DNA fragments—11 kb and 17 kb—in the magnetic trapping experiments, the fraction of molecules relaxed in a single burst remained similar to that calculated for 2-kb fragments (51% and 58%, respectively; Figure 4A). Even when the length of the DNA molecule was 51 kb (which allowed us to introduce up to 150 supercoils per molecule) in 49% of relaxation events nearly all supercoils were removed in a single burst, whilst for 51% of molecules we observed one or more pauses separating

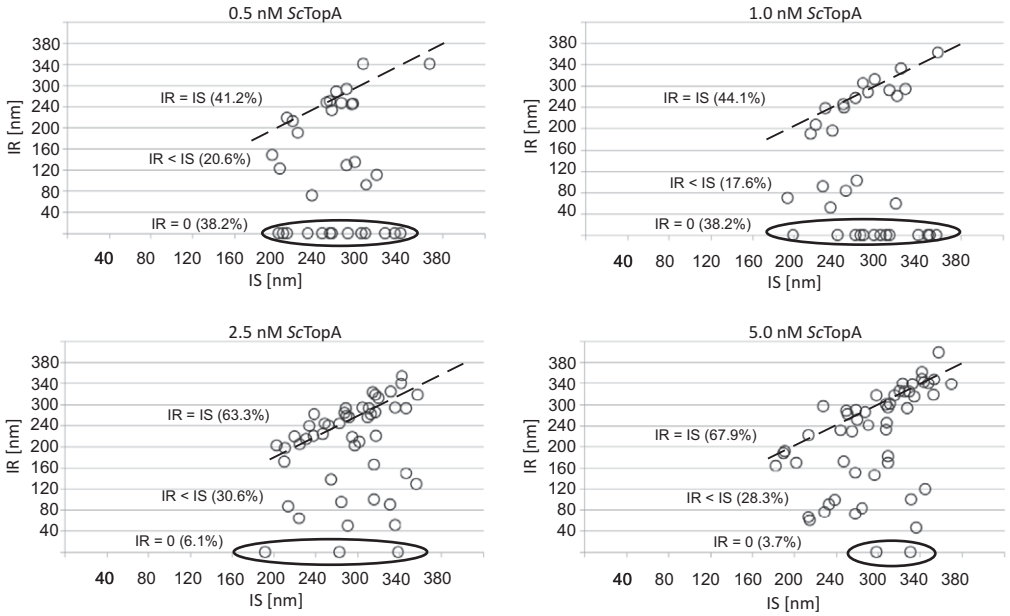

Figure 3. *Sc*TopA concentrations do not influence enzyme processivity. The enzyme processivity as expressed by the ratio between initial supercoiling (IS) and initial relaxation (IR). Each circle represents a single DNA relaxation event; circles accumulated near the dotted line correspond to nearly full relaxation of supercoiled DNA in single relaxation event (IS = IR), circles marked with a ellipse represent the fraction of DNA molecules remaining supercoiled (IR = 0 within the 800-s recording time); circles located in between correspond to molecules relaxed in more than one burst (IS > IR). Percentage of molecules belonging to each population are shown on each diagram in brackets.

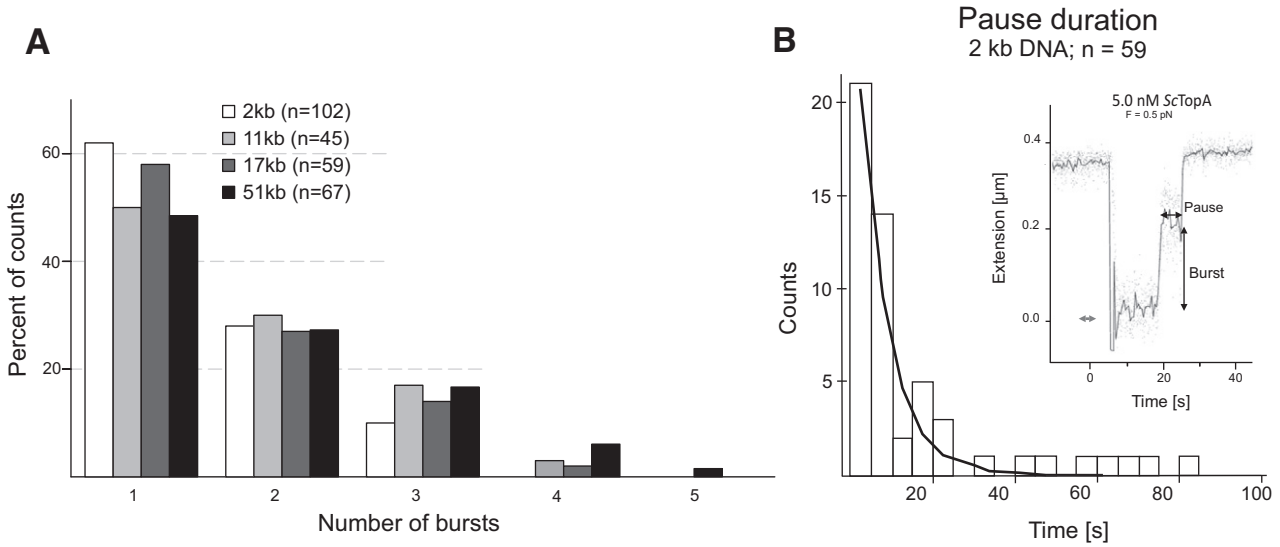

Figure 4. Relaxation bursts and pausing by *Sc*TopA. (**A**) The number of relaxation bursts required to remove negative supercoils from DNA is not dependent on the length of DNA substrates. Histograms show the fractions of 2–51-kb DNA molecules relaxed in the specified number of bursts (1–5). (**B**) Example of a pause between two successive relaxation bursts and distribution of pause lifetimes.

each burst. The pause duration between two bursts was calculated to be 10-fold shorter than the time necessary for reaction initiation (Figure 4B).

Independently of the length of the DNA substrate *Sc*TopA removes all negative supercoils from it in the first relaxation burst. However, we observed that occasionally the enzyme pauses during a relaxation burst and requires some time to start the next relaxation burst. Moreover, comparison of the ITLs and the pause duration suggests that during relaxation cycle *Sc*TopA does not dissociate form DNA, since the pause time is remarkably shorter than ITLs calculated for the same enzyme concentration.

*Sc*TopA exhibits higher processivity and velocity than other TopA homologues

Originally all type IA (29,30) topoisomerases were demonstrated to use a strand-passage mechanism to decrease gradually the superhelical density ($\Delta L_k = -1$) of negatively supercoiled DNA resulting in a distributive pattern of relax-

ation products. However, differences in the mechanism of relaxation of negatively supercoiled DNA between TopA and TopB (both belonging to the subtype IA) have recently been described (16–18). The ability of *Sc*TopA to remove a large number of supercoils in a single burst independently of enzyme concentration and substrate length prompted us to further explore its properties, in particular its reaction rate and processivity, using a long DNA fragment as substrate.

Reaction rates, given in μm/s, correspond to the speed at which the DNA extension increases as supercoils are removed by *Sc*TopA (Figure 5A), and the distribution of reaction rates is given in Figure 5B. The velocity distribution appears to be Gaussian, with a mean reaction rate of 0.45 μm/s. The reaction rate in units of supercoils (L_k) removed per second is obtained by dividing the reaction rate given in μm/s by the size of a single supercoil (~60 nm/supercoil in the experimental conditions used here), giving a mean on the order of 8–10 L_k/s (Figure 5B).

To estimate the processivity of the enzyme, we determined the number of supercoils (L_k) removed only in the first burst of *Sc*TopA activity; a plot of the resulting probability distribution is shown in Figure 5C. The distribution is characterized by a weak decay at small values as well as a 'brick wall' at 7.0 μm corresponding to relaxation events that are substrate-limited. Clearly the very high processivity of *Sc*TopA makes it difficult to quantify as even the longest single-molecule DNA substrate is too short for the processivity of most events to be determined. Although a significant number of events were observed for which the change in DNA extension was less than 7.5 μm and frequency of shorter bursts was constant (5–7% per 1 μm) suggesting the stochastic pause of relaxation process (Figure 5C), the most likely events corresponded to those for which nearly all supercoils were removed in the first burst of *Sc*TopA activity. We note that some measurements show more than 150 turns removed in one burst, which is presumably due to the fact that individual molecules can occasionally be only partially relaxed during a prior relaxation run. When supercoiled by an additional 150 negative turns, the population of molecules obtained thus includes some individuals with more negative supercoiling than the 150 added turns yet which can still be removed in a single burst of catalysis.

Three parameters (ITL, processivity and velocity) influence the overall reaction velocity. Based on the collected data, we calculated the average total relaxation rate (TRR) for two DNA substrates: 2-kb DNA and pUC19 (~2.7 kb) in single molecule and bulk experiments, respectively (Supplementary Figure S4A and B). TRR is defined by the time lapse between the mechanically introduced negative supercoils on DNA molecule to the point at which the bead returns to the starting position (as the result of enzyme activity). The TRR parameter calculated for 2 kb was similar (the values for most of them were not higher than 0.3 L_k/s) to the TRR_{bulk} calculated for pUC19 plasmid based on the Michaelis–Menten equation (0.2 L_k/s) (Supplementary Figure S4C). The comparison of relaxation patterns of two negatively supercoiled plasmids differing in length and linking number (L_k) shows that the *Sc*TopA relaxes both substrates with the same high processivity if the molar ratio of enzyme:plasmid is retained (Supplementary Figure S7). Thus, our results suggest that the overall relaxation velocity is the intrinsic property of the enzyme and is not dependent on the substrate type.

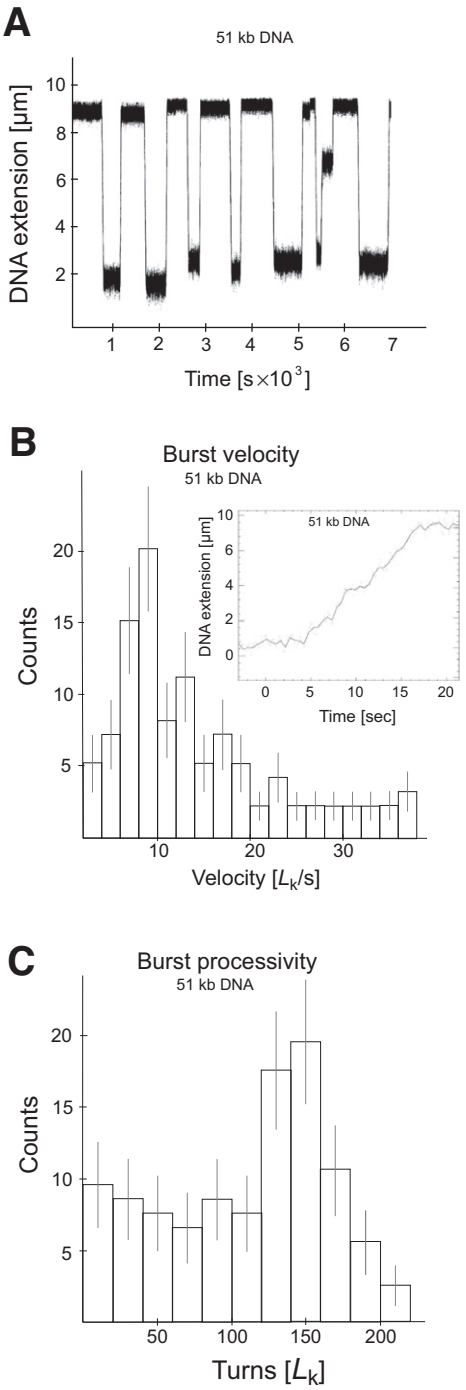

Figure 5. *Sc*TopA relaxation exhibits high velocity and processivity of supercoils removal (L_k/s) in a single burst. (**A**) Typical time-trace for supercoils relaxation as observed on 51-kb DNA substrate supercoiled by −150 turns. (**B**) Burst velocity distribution and (inset) expanded view of a relaxation burst. (**C**) Burst processivity distribution.

In summary, *Sc*TopA differs from its TopA homologue from *E. coli* in terms of both burst velocity of supercoil removal and processivity. Comparing with *E. coli* TopA, for which average velocity and processivity were estimated as

3.3 L_k/s and 20 L_k/run, respectively (16), *Sc*TopA is about 3-fold faster (10 L_k/s) and almost 10-fold more processive (150 L_k/burst). However, the waiting time preceding the supercoils removal by *Sc*TopA makes the overall enzyme less effective than if calculated only based on the burst velocity and processivity.

*Sc*TopA switches between processive and distributive DNA relaxation in a torque-dependent manner

To determine how efficient *Sc*TopA was at completely removing all supercoils, we measured the number of residual supercoils left unremoved by *Sc*TopA activity. This was done by initially supercoiling the DNA by a fixed number of turns, denoted by n, and determining the resulting extension of the molecule, denoted by l_1. After *Sc*TopA has been allowed to act on the DNA for a fixed amount of time, it is supercoiled anew by the same number of turns, n, and the resulting extension l_2 is recorded. This extension l_2 is systematically smaller than l_1 (Figure 6), indicating that there remained non-zero residual supercoiling after *Sc*TopA action. The difference in extensions l_2–l_1 is thus related to the number of residual, unrelaxed supercoils, n_{res}, according to $n_{res} = (l_2–l_1)/\delta$, where δ is the change in DNA extension associated with one supercoil.

We first determined the distribution of n_{res} for 17-kb substrate DNA supercoiled by −50 turns and allowed to react with *Sc*TopA for 250 s at a low extending force (F = 0.3 pN). In this timeframe, all molecules are nearly completely relaxed by one or more bursts of *Sc*TopA activity, however, as shown in Figure 6A, there remains on average 15 supercoils in the DNA. We next determined the distribution of n_{res} for the same DNA and the same IS, but allowing *Sc*TopA to react for 1000 s (Figure 6B). The latter distribution shows that allowing the enzyme to act for longer leads to a slightly smaller number of residual supercoils but comparing the two distributions indicates that the enzyme has lost nearly all of its processivity and is only able to remove a small number of supercoils at a time. We next repeated this experiment using 51-kb substrate DNA supercoiled by −150 turns and allowed to react for 250 s; the distribution of residual supercoiling is shown in Figure 6C. Comparing the data obtained with the shorter and longer DNA molecules shows that n_{res} is proportional to the length of the substrate DNA, as would be expected for a topoisomerase with torque-dependent processivity. In agreement with this, we found that when the first experiment in this series was repeated but for an increased extending force (F = 1 pN), the distribution of n_{res} became centred about n_{res} = 0 (Figure 6B, inset).

We also calculated the superhelical densities of 17-kb and 51-kb DNA at the point at which the *Sc*TopA processivity dropped as $\sigma_{17} = -0.008 \pm 0.001$ and $\sigma_{51} = 0.009 \pm 0.001$, respectively (Figure 6B and C). These results suggest that decreasing the absolute density below ∼0.01 inhibits enzyme processivity. From extension versus supercoiling curves (Supplementary Figure S7) we note that this supercoiling density corresponds to the buckling transition for DNA extended at this low force (F = 0.3 pN), and at this force the buckling transition occurs at a torque on the order of 4 pN·nm (or ∼1 k_BT) (31). This value is close to the denaturation torque for DNA, suggesting that the existence of denatured regions may be crucial to maintaining a high degree of processivity for *Sc*TopA.

To conclude, these data indicate that *Sc*TopA removes supercoils in a highly processive fashion as long as the torque acting on the DNA is high enough, but at low torques displays distributive activity.

Processivity of *Sc*TopA protein is provided by the positively charged C-terminus

*Sc*TopA processivity was also analysed by resolving the reaction intermediates in agarose gel electrophoresis. In this assay, a broad range of enzyme concentrations (0–150 nM) was used in reactions with negatively supercoiled pUC19 plasmid. *Sc*TopA-mediated plasmid relaxation led to appearance of low-density topoisomers even when supercoiled plasmid or its partially relaxed topoisomers were still noticeable (Figure 7A) confirming the processive behaviour of *Sc*TopA and underscoring the difference in relaxation mechanism between *Sc*Top protein and its homologue from *E. coli*. The presence of positively charged amino acids at the C-terminal end of *Sc*TopA prompted us to analyse the DNA relaxation properties of mutants lacking either the whole C-terminal domain (343 aa; *Sc*TopAΔC) or the stretch of basic amino acids at the C-terminus (71 aa; *Sc*TopA881). Interestingly, removal of the whole C-terminal domain almost completely abolished enzyme activity (Figure 7D), whilst the pattern of *Sc*TopA881 relaxation products was distributive (Figure 7B, left panel) instead of processive as observed for the wild-type protein (Figure 7B, right panel). By titrating the pUC19 reaction substrate from 10 to 70 nM, we measured the reaction velocities for *Sc*TopA and *Sc*TopA881 within their linear range and fitted the reaction kinetics to the Michaelis–Menten model (see the Materials and Methods section). Based on differential equation of the model, the maximal enzymatic rates V_{max} were calculated to be 6.5 nM/min for 5-nM *Sc*TopA and Michaelis–Menten constant K_m 5.1 nM and 0.62 nM/min and 20.7 nM, respectively, for the mutant *Sc*TopA881 (Figure 7C).

In summary, these bulk experiments confirm the high processivity of *Sc*TopA and demonstrate that complete removal of the C-terminal domain abolishes enzyme activity whilst truncation of its positively charged C-terminus affects affinity for substrate and processivity.

DISCUSSION

Many bacteria, especially rapidly growing species (*E. coli*, *Bacillus subtilis*), possess two topoisomerases of type IA– –topoisomerase I (TopA) and topoisomerase III (TopB). In contrast, *Actinobacteria* possess only one gene encoding a type IA topoisomerase, TopA. Although in *E. coli* both proteins TopA and TopB are closely related and share the same catalytic mechanism, they relax DNA with different efficiencies and processivities and play key roles in different cellular processes (16,32–34). Sequence and structure alignments suggest that *S. coelicolor* TopA (*Sc*TopA), similar to homologous *M. smegmatis* TopA (*Ms*TopA), possesses a unique C-terminal domain that terminates with a

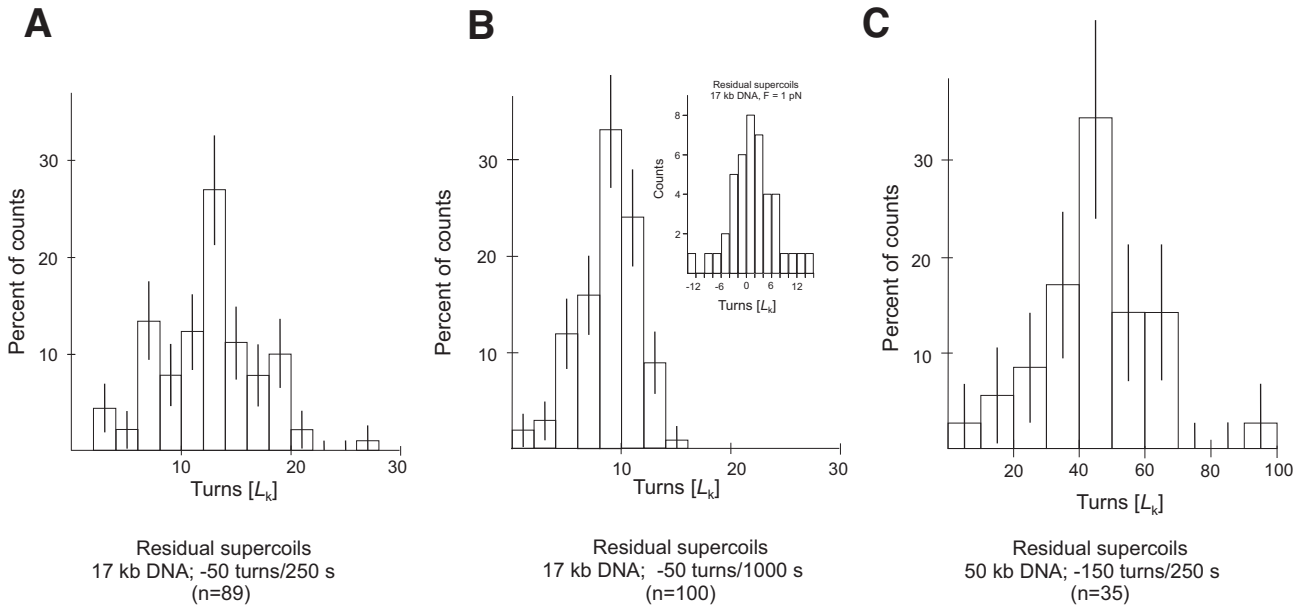

Figure 6. Residual supercoiling left unremoved by *Sc*TopA relaxation bursts indicates *Sc*TopA switches between high and low processivity as a function of torque acting on the DNA. Seventeen-kilobase DNA supercoiled by −50 turns and left to react with TopA shows (**A**) relaxation of ∼38 supercoils in the first 250 s of incubation but only (**B**) relaxation of ∼3 additional supercoils in the following 750 s of the reaction, for an extending force of about 0.3 pN. (Inset) When the extending force is increased to 1 pN, the average residual supercoiling is zero after a 250-s reaction. (**C**) Fifty-one-kilobase DNA supercoiled by −150 turns and left to react with TopA for 250 s shows an increase in residual supercoils roughly three times greater than what is observed on 17-kb DNA.

Table 1. Characterization of DNA relaxation by type I topoisomerases: *E. coli* (*Ec*TopA and *Ec*TopB), human type IB topoisomerase and *S. coelicolor* (*Sc*TopA)

Parameter	*Ec*TopA	*Ec*TopB	Human type IB topo	*Sc*TopA
Relaxation rate per burst (L_k/s)	3.3	129	134	8
Initial time lag (ITL)[a] (s)	1.6	129	nd	29
Turns removed in a single burst (L_k) (low torque)	20	28	50	150[b]

[a]ITL was estimated for 2-nM *Sc*TopA and was compared with 2-nM *Ec*TopA and 2-nM *Ec*TopB (16).
[b]The number of turns removed by *Sc*TopA in a single relaxation burst may be higher than 150 L_k as the experimental estimation is limited by the 51-kb DNA substrate.

stretch of positively charged amino acids but which, unlike *E. coli* TopA, lacks Zn fingers (22,23). In contrast to previous observations made by Bao and Cohen (20), who reported a slightly decreased relaxation activity of *Sc*TopA protein lacking the C-terminal domain, our data show that removal of the C-terminal domain of *Sc*TopA completely abolished enzyme activity. Although our *Sc*TopAΔC mutant (lacking 343 aa) and the mutant constructed by Bao and Cohen (20) (lacking 353 aa) differ somewhat in length, it is difficult to explain the discrepancy in the observed enzyme activity. Interestingly, Jain and Nagaraja (35) demonstrated that the activity of *Ms*TopA lacking the C-terminal 34 kDa domain was also abolished; however, it could be restored if supplemented with recombinant C-terminal domain. Our studies showed that removal of the short positively charged C-terminus (71 aa) from *Sc*TopA greatly affected enzyme activity, reducing its processivity and affinity for the substrate. It has been proposed that basic amino acids may replace Zn fingers in efficient DNA binding and that their elimination decreases enzyme affinity for DNA substrates (36). Recently, Ahmed *et al.* (37) have shown that the C-terminal domain of *Ms*TopA protein may play a role in strand-passage and suggested that the presence of a positively charged C-terminus may provide an additional binding site, ensuring efficient DNA relaxation. Our calculation of K_m for the wild-type and truncated *Sc*TopA protein (5.1 and 20.7 nM, respectively) corroborates with this notion. It was earlier reported that *M. smegmatis Ms*TopA binds both single- and double-stranded DNA oligomers with similar affinity, and Mg^{2+} ions are not necessary for DNA binding and cleavage (24), however their concentration affected processivity of the enzyme (23). We also found that, although *Sc*TopA requires the presence of single-stranded regions in a substrate for relaxation, it effectively binds to double-stranded DNA (dsDNA) (Supplementary Figure S5).

Our results show that *Sc*TopA is able to remove up to 150 supercoils per relaxation burst and that the enzyme is characterized by a torque-dependent processivity which leads to more distributive and/or lower activity at low torque when most of the DNA supercoiling has been relaxed. The apparent processivity of *Sc*TopA could be the result of either simultaneous action of many protein molecules on DNA

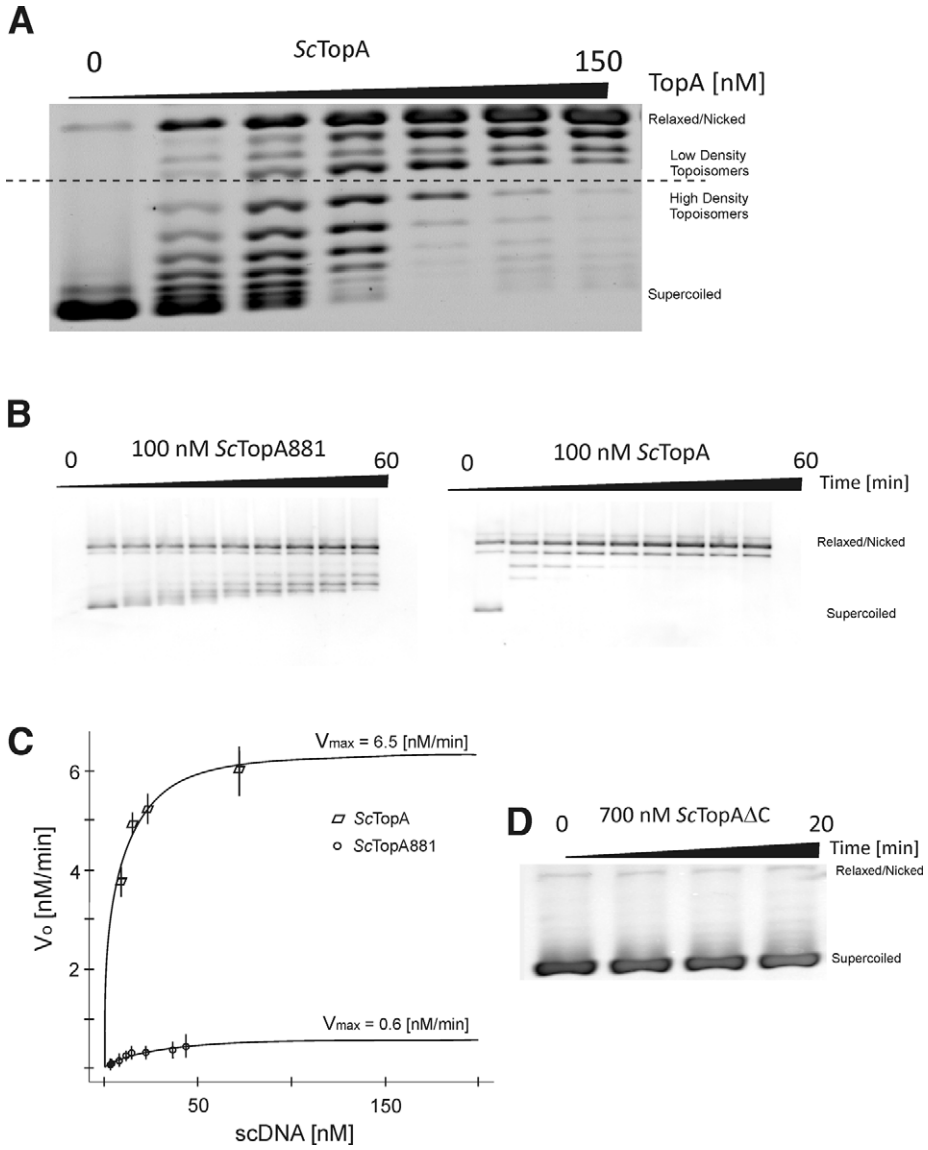

Figure 7. The relaxation of negatively supercoiled pUC19 plasmid by *Sc*TopA is dependent on its C-terminal domain. (**A**) Agarose gel-based assay demonstrating rapid appearance of low-density topoisomers produced by *Sc*TopA even at low protein concentration (25–50 nM; lanes 1 and 2). (**B**) Comparison of processive and distributive removal of supercoils during the reaction sustained by wild-type *Sc*TopA (100 nM) and mutant *Sc*TopA881 truncated in C-terminus by 71 amino acids (100 nM), respectively. (**C**) Estimation of kinetic parameters V_{max} and K_m by fitting to the Michaelis–Menten equation for wild-type *Sc*TopA and mutant *Sc*TopA881. (**D**) Deletion of C-terminal domain (343 aa) completely abolishes the activity of the *Sc*TopAΔC mutant (700 nM).

or the ability of a single *Sc*TopA molecule or multimeric complex to remove several supercoils each time it binds to DNA. Analysis of the concentration dependence of the reaction rules out the possibility that apparent processivity is due to multiple active complexes acting independently as processive activity was observed at all concentrations tested. The formation of a multimeric complex composed of many *Sc*TopA molecules acting and removing supercoils cooperatively could explain the long ITL observed for low *Sc*TopA concentration (conditions in which a long ITL could be due to shifting the complex-assembly equilibrium towards an inactive monomeric state). It has been reported earlier that vaccinia virus topoisomerase IB is able to form a filament spreading along dsDNA forming synapses between distinct DNA fragments in a highly cooperative fashion (38). Detailed analysis of enzyme activity supports the idea that a single *Sc*TopA molecule is able to act processively, although the hypothesis of multimer assembly cannot be excluded. The burst rate of supercoil removal by *Sc*TopA was determined to be 8 L_k/s, comparable to *E. coli* TopA (3.3 L_k/s) but significantly lower than that of *E. coli* TopB (129 L_k/s) or human type IB topoisomerase (6.7 μm/s; which corresponds to 134 L_k/s) (12,16). Nevertheless, the overall relaxation velocity results from the combination of the burst rate and the processivity related to affinity to substrate. Our single-molecule studies show that efficient DNA relaxation by *Sc*TopA is the result of extremely high processivity (150 L_k/burst), much higher than reported for *E. coli*

TopB (28 L_k/burst) and human TopIB (50 L_k/burst) estimated at similar extending force (12,16). *E. coli* TopB acts more processively than *E. coli* TopA presumably thanks to the creation of a stable enzyme:DNA complex (17,39) (Table 1). The high processivity of *Ec*TopB was linked to the presence of the positively charged region known as the decatenation loop in its N-terminal domain (17). Disruption of the decatenation loop resulted in inhibition of the enzyme via an apparent reduction in processivity. *Sc*TopA does not possess a bona fide decatenation loop, although some homologous amino acids are present in its N-terminal domain (Supplementary Figure S1D). Thus, increased enzyme processivity is presumably linked to the C-terminal stretch of basic amino acids as indicated by Ahmed *et al.* (37). Predictions of secondary structure suggest that the C-terminus of *Sc*TopA forms an α-helix with basic amino acids precisely oriented in a helical fashion on the surface of the α-helix and which may constitute the domain interacting with the highly compacted supercoiled DNA, providing higher affinity to substrate. This could confer the ability of a single *Sc*TopA molecule to remove several supercoils each time it binds to DNA and leading to processive removal of supercoils. Thus, our most favoured hypothesis explaining rapid removal of several supercoils is the formation of a stable and processive *Sc*TopA:DNA complex, perhaps thanks to the presence of denatured regions in the DNA.

In summary, we suggest that in *Streptomyces*, which lacks a copy of the *topB* gene encoding for topoisomerase III, *Sc*TopA exhibits some of the properties of TopA and TopB proteins. Although the portfolio of topology-modifying enzymes in *S. coelicolor* is simplified in comparison with other species, the topological problems it encounters during replication and segregation of a large number of long, linear chromosomes are presumably non-trivial. This could lead to the requirement for a highly processive topoisomerase, and indeed such features have been observed *in vitro* using bulk and single molecule techniques. The unusually high processivity of *Sc*TopA combined with its previously demonstrated telomerase activity (20) and its ability to resolve topological problems during chromosome segregation (21) suggests specific adaptation of the only type I topoisomerase in *S. coelicolor* to efficiently fulfil multiple functions.

SUPPLEMENTARY DATA

Supplementary Data are available at NAR Online.

ACKNOWLEDGEMENTS

The authors acknowledge financial support from the Parent Bridge Programme of Foundation for Polish Science, co-financed by European Union, Regional Development Fund, and from EURYI.

Authors Contributions: M.J.S. contributed substantially to conception and design, acquisition of data, analysis and interpretation of data and drafting the article. T.S. contributed substantially to conception and design, acquisition of data, or analysis and interpretation of data and revising the manuscript critically for important intellectual content. A.S. contributed to acquisition of data. J.Z.C. contributed to revising the manuscript critically for important intellectual content. D.J. contributed substantially to conception and design, drafting the article and final approval of the version to be published.

FUNDING

Parent Bridge Programme of Foundation for Polish Science; co-financed by European Union, Regional Development Fund; EURYI [to T.S.]. Funding for open access charge: Parent Bridge Programme of Foundation for Polish Science (POMOST/2010-2/5).

Conflict of interest statement. None declared.

REFERENCES

1. Everid,A.C., Small,J.V. and Davies,H.G. (1970) Electron-microscope observations on the structure of condensed chromatin: evidence for orderly arrays of unit threads on the surface of chicken erythrocyte nuclei. *J. Cell Sci.*, **7**, 35–48.
2. Richmond,T.J. and Davey,C.A. (2003) The structure of DNA in the nucleosome core. *Nature*, **423**, 145–150.
3. Zimmerman,S.B. (2006) Cooperative transitions of isolated Escherichia coli nucleoids: implications for the nucleoid as a cellular phase. *J. Struct. Biol.*, **153**, 160–175.
4. Zimmerman,S.B. (2006) Shape and compaction of Escherichia coli nucleoids. *J. Struct. Biol.*, **156**, 255–261.
5. Nasmyth,K. and Haering,C.H. (2005) The structure and function of SMC and kleisin complexes. *Annu. Rev. Biochem.*, **74**, 595–648.
6. Carter,S.D. and Sjögren,C. (2012) The SMC complexes, DNA and chromosome topology: right or knot? *Crit. Rev. Biochem. Mol. Biol.*, **47**, 1–16.
7. Thadani,R., Uhlmann,F. and Heeger,S. (2012) Condensin, chromatin crossbarring and chromosome condensation. *Curr. Biol.*, **22**, R1012–R1021.
8. Champoux,J.J. (2001) DNA topoisomerases: structure, function, and mechanism. *Annu. Rev. Biochem.*, **70**, 369–413.
9. Forterre,P. and Gadelle,D. (2009) Phylogenomics of DNA topoisomerases: their origin and putative roles in the emergence of modern organisms. *Nucleic Acids Res.*, **37**, 679–692.
10. Forterre,P., Gribaldo,S., Gadelle,D. and Serre,M.C. (2007) Origin and evolution of DNA topoisomerases. *Biochimie*, **89**, 427–446.
11. Belova,G.I., Prasad,R., Nazimov,I.V., Wilson,S.H. and Slesarev,A.I. (2002) The domain organization and properties of individual domains of DNA topoisomerase V, a type 1B topoisomerase with DNA repair activities. *J. Biol. Chem.*, **277**, 4959–4965.
12. Koster,D.A., Croquette,V., Dekker,C., Shuman,S. and Dekker,N.H. (2005) Friction and torque govern the relaxation of DNA supercoils by eukaryotic topoisomerase IB. *Nature*, **434**, 671–674.
13. Seol,Y., Zhang,H., Pommier,Y. and Neuman,K.C. (2012) A kinetic clutch governs religation by type IB topoisomerases and determines camptothecin sensitivity. *Proc. Natl. Acad. Sci. U.S.A.*, **109**, 16125–16130.
14. Aravind,L., Leipe,D.D. and Koonin,E.V. (1998) Toprim–a conserved catalytic domain in type IA and II topoisomerases, DnaG-type primases, OLD family nucleases and RecR proteins. *Nucleic Acids Res.*, **26**, 4205–4213.
15. Cheng,B., Sorokin,E.P. and Tse-Dinh,Y.C. (2008) Mutation adjacent to the active site tyrosine can enhance DNA cleavage and cell killing by the TOPRIM Gly to Ser mutant of bacterial topoisomerase I. *Nucleic Acids Res.*, **36**, 1017–1025.
16. Terekhova,K., Gunn,K.H., Marko,J.F. and Mondragón,A. (2012) Bacterial topoisomerase I and topoisomerase III relax supercoiled DNA via distinct pathways. *Nucleic Acids Res.*, **40**, 10432–10440.
17. Li,Z., Mondragón,A., Hiasa,H., Marians,K.J. and DiGate,R.J. (2000) Identification of a unique domain essential for Escherichia coli DNA topoisomerase III-catalysed decatenation of replication intermediates. *Mol. Microbiol.*, **35**, 888–895.
18. Nurse,P., Levine,C., Hassing,H. and Marians,K.J. (2003) Topoisomerase III can serve as the cellular decatenase in Escherichia coli. *J. Biol. Chem.*, **278**, 8653–8660.
19. Bentley,S.D., Chater,K.F., Cerdeño-Tárraga,A.M., Challis,G.L., Thomson,N.R., James,K.D., Harris,D.E., Quail,M.A., Kieser,H. and

Harper,D. (2002) Complete genome sequence of the model actinomycete Streptomyces coelicolor A3(2). *Nature*, **417**, 141–147.
20. Bao,K. and Cohen,S.N. (2004) Reverse transcriptase activity innate to DNA polymerase I and DNA topoisomerase I proteins of Streptomyces telomere complex. *Proc. Natl. Acad. Sci. U.S.A.*, **101**, 14361–14366.
21. Szafran,M., Skut,P., Ditkowski,B., Ginda,K., Chandra,G., Zakrzewska-Czerwińska,J. and Jakimowicz,D. (2013). Topoisomerase I (TopA) is recruited to ParB complexes and is required for proper chromosome organization during Streptomyces coelicolor sporulation. *J. Bacteriol.*, **195**, 4445–4455.
22. Bhaduri,T. and Nagaraja,V. (1994) DNA topoisomerase I from Mycobacterium smegmatis. *Indian J. Biochem. Biophys.*, **31**, 339–343.
23. Bhaduri,T., Bagui,T.K., Sikder,D. and Nagaraja,V. (1998) DNA topoisomerase I from Mycobacterium smegmatis. An enzyme with distinct features. *J. Biol. Chem.*, **273**, 13925–13932
24. Bhaduri,T., Sikder,D. and Nagaraja,V. (1998) Sequence specific interaction of Mycobacterium smegmatis topoisomerase I with duplex DNA. *Nucleic Acidc Res.*, **26**, 1668–1674.
25. Xu,X. and Leng,F. (2011) A rapid procedure to purify Escherichia coli DNA topoisomerase I. *Protein Expr. Purif.*, **77**, 214–219.
26. Revyakin,A., Ebright,R.H. and Strick,T.R. (2005) Single-molecule DNA nanomanipulation: improved resolution through use of shorter DNA fragments. *Nat. Methods*, **2**, 127–138.
27. Charvin,G., Vologodskii,A., Bensimon,D. and Croquette,V. (2005) Braiding DNA: experiments, simulations, and models. *Biophys. J.*, **88**, 4124–4136.
28. Strick,T.R., Allemand,J.F., Bensimon,D., Bensimon,A. and Croquette,V. (1996) The elasticity of a single supercoiled DNA molecule. *Science*, **271**, 1835–1837.
29. Dean,F.B. and Cozzarelli,N.R. (1985) Mechnism of strand passage by Escherichia coli topoisomerase I. The role of the required nick in catenation and knotting of duplex DNA. *J. Biol. Chem.*, **260**, 4984–4994.
30. Dekker,N.H., Rybenkov,V.V., Duguet,M., Crisona,N.J, Cozzarelli,N.R., Bensimon,D. and Croquette,V. (2002) The mechanism of type IA topoisomerases. *Proc. Natl. Acad. Sci. U.S.A.*, **99**, 12126–12131.
31. Mosconi,F., Allemand,J.F., Bensimon,D. and Croquette,V. (2009) Measurement of the torque on a single stretched and twisted DNA using magnetic tweezers. *Phys. Rev. Lett.*, **102**, 078301.
32. Ahumada,A. and Tse-Dinh,Y.C. (2002) The role of the Zn(II) binding domain in the mechanism of E. coli DNA topoisomerase I. *BMC Biochem.*, **3**, 1–13.
33. Vos,S.M., Tretter,E.M., Schmidt,B.H. and Berger,J.M. (2011) All tangled up: how cells direct, manage and exploit topoisomerase function. *Nat. Rev. Mol. Cell Biol.*, **12**, 827–841.
34. Perez-Cheeks,B.A., Lee,C., Hayama,R. and Marians,K.J. (2012) A role for topoisomerase III in Escherichia coli chromosome segregation. *Mol. Microbiol.*, **86**, 1007–1022.
35. Jain,P. and Nagaraja,V. (2006) Indispensable, functionally complementing N and C-terminal domains constitute site-specific topoisomerase I. *J. Mol. Biol.*, **357**, 1409–1421.
36. Zhang,Z., Cheng,B. and Tse-Dinh,Y.C. (2011) Crystal structure of a covalent intermediate in DNA cleavage and rejoining by Escherichia coli DNA topoisomerase I. *Proc. Natl. Acad. Sci. U.S.A.*, **108**, 6939–6944.
37. Ahmed,W., Bhat,A.G., Leelaram,M.N., Menon,S. and Nagaraja,V. (2013) Carboxyl terminal domain basic amino acids of mycobacterial topoisomerase I bind DNA to promote strand passage. *Nucleic Acids Res.*, **41**, 7462–7471.
38. Moreno-Herrero,F., Holtzer,L., Koster,D.A., Shuman,S., Dekker,C. and Dekker,N.H. (2005) Atomic force microscopy shows that vaccinia topoisomerase IB generates filaments on DNA in a cooperative fashion. *Nucleic Acids Res.*, **33**, 5945–5953.
39. Zhang,H.L. and DiGate,R.J. (1994) The carboxyl-terminal residues of Escherichia coli DNA topoisomerase III are involved in substrate binding. *J. Biol. Chem.*, **269**, 9052–9059.